NASA Technical Paper 2904

1989

Design, Fabrication, and Performance of Brazed, Graphite Electrode, Multistage Depressed Collectors With 500-W, Continuous Wave, 4.8- to 9.6-GHz Traveling-Wave Tubes

Peter Ramins
and Ben Ebihara
Lewis Research Center
Cleveland, Ohio

National Aeronautics and Space Administration
Office of Management
Scientific and Technical Information Division

Summary

A small, isotropic graphite electrode, multistage depressed collector (MDC) was designed, fabricated, and evaluated in conjunction with a 500-W, continuous wave (CW), 4.8- to 9.6-GHz traveling-wave tube (TWT). The carbon electrode surfaces were used to improve the TWT overall efficiency by minimizing the secondary-electron-emission losses in the MDC. The design and fabrication of the brazed graphite MDC assembly are described. The brazing technique, which used copper braze filler metal, is compatible with both vacuum and the more commonly available hydrogen atmosphere brazing furnaces. The TWT and graphite electrode MDC bakeout, processing, and outgassing characteristics were evaluated and found to be comparable to TWT's equipped with copper electrode MDC's. The TWT and MDC performance was optimized for broadband CW operation at saturation. The average radiofrequency (RF), overall, and MDC efficiencies were 14.9, 46.4, and 83.6 percent, respectively, across the octave operating band. A 1500-hr CW test, conducted without the use of an appendage ion pump, showed no gas buildup and excellent stability of the electrode surfaces.

Introduction

A promising new multistage depressed collector (MDC) electrode material, a particular form of isotropic graphite manufactured by POCO Graphite, Inc., (DFP–2) was reported in references 1 to 3. The low secondary-electron-emission yield carbon electrode surfaces produced a very significant improvement in the traveling-wave tube (TWT) overall and MDC efficiencies, as compared with TWT's equipped with copper electrode MDC's (ref. 4). Because of compatible thermal expansion characteristics, the isotropic graphite electrodes could be brazed directly to the electrical insulators, thereby enabling the following:

(1) Elimination of ceramic-to-metal braze interfaces which serve as vacuum seals
(2) Simple and effective conduction cooling of the electrodes
(3) Achievement of very compact MDC assemblies

However, the brazing techniques originally devised for the graphite required a special (vacuum) furnace, since the braze filler metal contained an active metal (titanium) which is not compatible with the commonly available (and rapidly cycled) hydrogen atmosphere brazing furnaces. Moreover, the major constituent of the braze filler metal was silver, an undesirable material for long-life TWT's. Furthermore, only limited information was available on the extent (if any) to which the graphite electrode MDC's would require (1) special (or extended) bakeout, (2) additional processing time, or (3) continued use of appendage pumps.

These important considerations, which could limit the practicality and extent of use of the graphite MDC's, were addressed in the subsequent technology demonstration program described in this paragraph. Computer-aided design techniques (ref. 1) were used to design a small-sized MDC for a representative TWT. A high-temperature brazing technique, compatible with both vacuum and hydrogen brazing furnaces, was devised, and complete isotropic graphite MDC assemblies were fabricated and added to TWT bodies. The TWT-MDC's were put through a typical production-line sequence of bakeout and gradual processing (outgassing). The performance of one of the TWT's was subsequently optimized and evaluated. This report presents the following:

(1) Description of the improved brazing technique
(2) Outgassing performance of the graphite MDC's during bakeout and processing, as compared with the same model TWT's equipped with copper electrode MDC's
(3) Evaluation of the stability of the carbon electrode surfaces over an extended period of continuous wave (CW) operation
(4) CW performance of the TWT-MDC and a comparison of the predicted (analytical) and measured MDC performance

The authors wish to express their gratitude to Eric Nettesheim of Teledyne MEC for documentation of the TWT-MDC outgassing performance during the bakeout and subsequent processing, and to Dale A. Force of the NASA Lewis Research Center for analyzing the performance of the MDC.

Symbols

I_B intercepted beam current in forward direction, A

I_{en} net current to collector electrode n, A

I_G total body current, including backstreaming from collector, A

I_0 beam current, A

P_b body power, sum of RF circuit losses and intercepted beam power in forward direction, W

P_{col} collector power, $V_0 I_0 - P_{RF} - P_b$, W

P_{rec} recovered power, $\sum_{n=1}^{4} V_{en}I_{en}$, W

P_{RF} total RF output power, W

P' prime power, $V_0 I_G + \sum_{n=1}^{4} (V_0 - V_{en})I_{en}$, W

V_{en} voltage on collector electrode n with respect to ground, V

V_0 cathode potential with respect to ground, V

η_c TWT circuit efficiency, $P_{RF}/(P_{RF}$ + circuit losses), percent

η_{col} collector efficiency, P_{rec}/P_{col}, percent

η_e electronic efficiency, η_{RF}/η_c

η_{ov} TWT overall efficiency, P_{RF}/P', percent

η_{RF} RF efficiency of TWT, $P_{RF}/V_0 I_0$, percent

Design, Fabrication, and Performance Evaluation Program

Overall Program

The program included the evaluation of the outgassing performance, from bakeout to the achievement of CW operation, of three Teledyne MEC model MTH-5065 TWT's equipped with NASA Lewis furnished isotropic graphite MDC's. These will be referred to as TWT's 004 to 006 throughout this report. One of these (TWT 004) was selected for extensive performance optimization and evaluation at NASA Lewis. The MDC's were designed and assembled at NASA Lewis. Certain MDC components were fabricated at NASA; others were obtained by using outside (contracted) fabrication services. The design effort included both the active (electrode geometry) and the passive electrode support structure (including cooling, high-voltage (HV) standoff, and vacuum envelope designs) of the MDC.

The MDC's were joined to the TWT bodies, baked out, focused, and brought up to the CW operation at Teledyne MEC. The bakeout performance and the early processing performance were noted in a log supplied by Teledyne MEC with each tube. The final focusing and the optimization and evaluation of the performance of TWT 004 were performed at NASA Lewis.

This program was a continuation of that reported in reference 5 (wherein the RF performance of TWT model MTH-5065, serial number 001, is described). The MDC geometric design, however, was improved to reduce backstreaming current from the MDC electrodes by better electrostatic suppression of secondary electrons. Moreover, TWT's 004 to 006 had electron guns of improved design.

TWT, Refocuser, and MDC Characteristics

The general characteristics of TWT 004 are shown in table I. This model is a medium-power, CW, helical TWT with RF output and spent beam powers well above those of typical space TWT's. This model is nominally a dual-mode tube with a relatively small (2 dB) pulse-up capability in RF output power. The average levels of parameters wuch as prime power P', total RF output power P_{RF}, collector power P_{col}, and the MDC dissipation, however, are highest for the CW mode, since the duty cycle in the pulsed-up mode is limited to 50 percent. Consequently, the TWT-MDC was optimized for the CW (high stress) mode, and testing at NASA Lewis was limited to the CW mode. The TWT-MDC had a 2-liter/s ion pump at the MDC and a small (0.2-liter/s) appendage pump at the electron gun. It was anticipated that the larger ion pump would be used only during the processing phase to minimize the time required to bring the TWT-MDC up to CW operation with subsequent pumping (if any) being performed by the appendage pump.

The spent beam refocuser consisted of two full-strength permanent magnets (in a continuation of the periodic permanent magnet (PPM) stack) past the RF output of the TWT, and required only the addition of a single magnet to the output end of the production TWT.

The geometry of the active portion of the MDC, the typical operating potentials, and the charge trajectories are shown in figure 1. The trajectories and the computed collector performance are discussed in a subsequent section of this report (Comparison of Computed and Measured Results). The isotropic graphite collector electrodes of the TWT's 005 and 006 were used in the "as-machined" state; those of TWT 004 were lightly blasted with 50-μm alumina particles to further improve the collector and TWT overall efficiencies, η_{col} and η_{ov}, respectively (ref. 4). The MDC assemblies were designed to fit within the envelope of the existing production-model TWT's, and to be conductively cooled to the same baseplate.

TABLE I.—GENERAL CHARACTERISTICS OF TELEDYNE MEC TWT MODEL MTH-5065 (TWT 004)

Frequency, GHz	4.8 to 9.6
Cathode potential, V_0, kV	9.75
Beam current, I_0,A	0.362
Perveance, A/V$^{3/2}$	0.38×10^{-6}
RF output power, P_{RF}, W	600 (Maximum)
Focusing	Periodic permanant magnet (PPM)
Duty cycle, percent	100

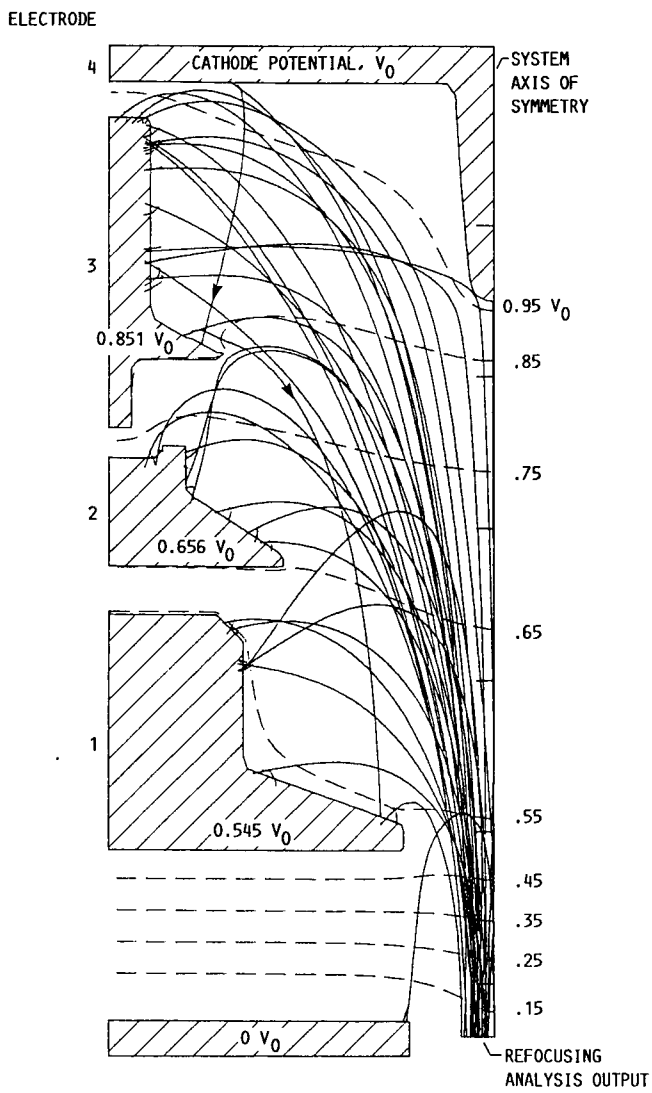

Figure 1.—Active geometry and trajectories of primary- and secondary-electron-emission charges in four-stage, 2.4-cm-diameter collector. TWT operating at saturation at 8.4 GHz in low mode.

MDC Assembly Design and Fabrication

Basic Electrode Material

The collector electrodes were made of POCO Graphite, Inc., grade DFP–2 isotropic graphite, which is an ultrafine-grain, high-purity, readily machinable material having other distinctive advantages as well (Data sheet for DFP–2, Semiconductors Metallurgical Grades, POCO Graphite, Inc., Decatur, Texas, January 1, 1978). The material has an open and interconnecting porosity, which expedites outgassing during vacuum bakeout. Its coefficient of thermal expansion is such that direct brazing to alumina (and beryllia) is possible. The impurity level is less than 5-ppm ash content. It has relatively good (low) secondary-electron-emission characteristics from machined surfaces, and can be readily textured to produce a surface with extremely low secondary-electron-emission characteristics (ref. 2).

MDC Assembly Design and Fabrication

In general, the fabrication techniques and the modular design concept described in detail in reference 3 were used. The brazing technique used to join the graphite to the alumina insulators, however, was modified to (1) make all brazing and any heat-treating operations compatible with hydrogen atmosphere furnaces, (2) replace the silver-base, active-metal braze filler alloy (Ticusil) with copper, and (3) simplify the production of the MDC modules by eliminating multiple braze operations (unpublished research by Ben Ebihara, NASA Lewis Research Center, Cleveland, Ohio).

These changes were made possible by a metalization technique, in which a thin coating of a metal powder slurry (containing molybdenum, manganese, and silica as major constituents) was brush-painted on the graphite, dried, and fired in a reducing atmosphere. The high-temperature (1600 °C) firing operation in dry hydrogen was performed to reduce any oxides in the metalization and to ensure adherent bond formation with the graphite by reactions with the elemental metalization constituents to form carbides. The scanning electron microscope photomicrograph of a typical cross section of metalized graphite, shown in figure 2, indicates good coverage and adhesion of the metalization. Further investigations are necessary, however, to optimize and explain the bond formation since there are many unknown variables as to material characteristics and processing parameters.

Figure 3 shows a schematic cross section of a typical module ready for brazing, including all the components and the necessary fixturing. The metalized outer circumferential surface of the tapered graphite plugs was overlaid with a thin copper coating, which served the dual functions of providing the required braze filler material and protecting the molybdenum-manganese metalization from oxidation. The alumina insulator ring was metalized on both its inner and outer circumferential surfaces.

Such metalized components can be joined by using standard brazing practices. Copper was selected for the braze filler material because of its ductility and compatibility with the commonly available (and rapid throughput) hydrogen atmosphere brazing furnaces. Moreover, both brazes (Kovar to alumina and alumina to graphite) can be made in a single operation.

A typical finished electrode module is shown in figure 4. Final machining of the graphite to the required electrode shape was done after completion of the braze operation. The edges of the outer ring of the electrode modules and the electrical feedthrough element were prepared with matching butt-lap joints to provide self-fixturing weld connections and concentric alignment of the electrodes. The individual components which

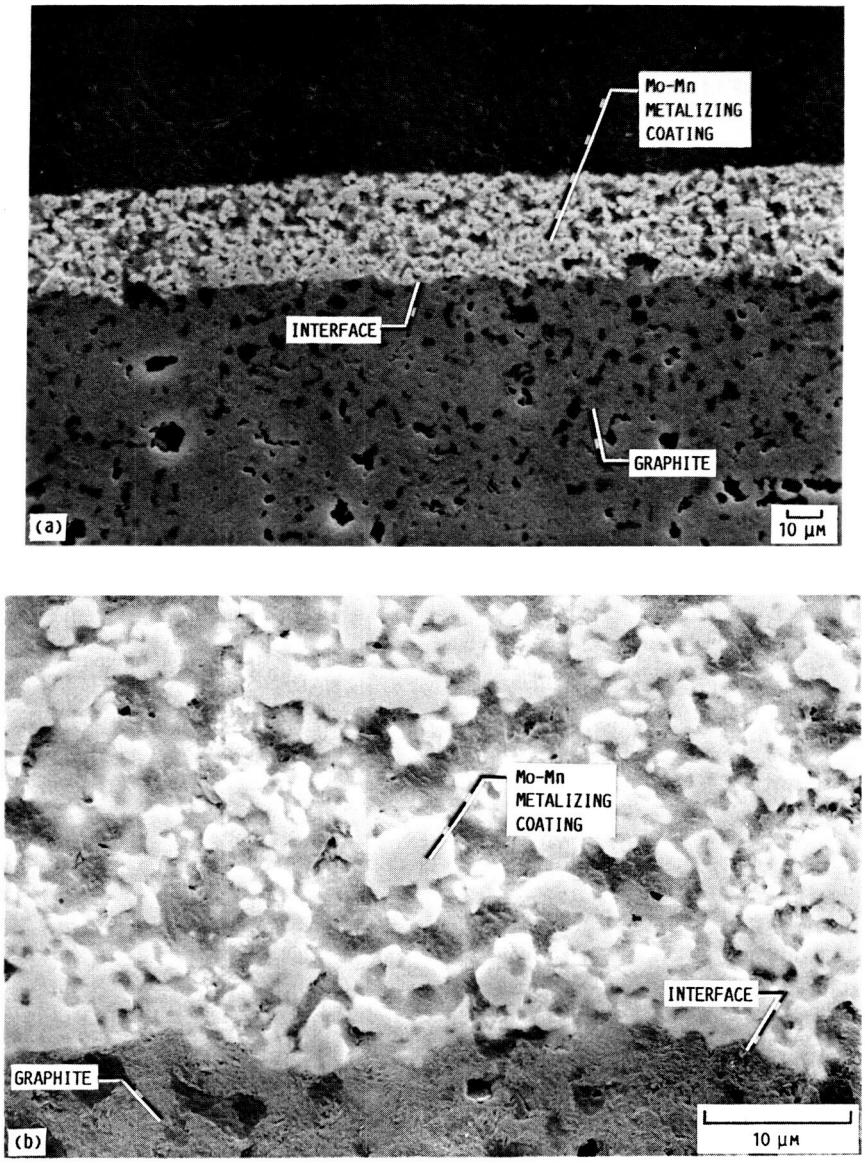

(a) Coating cross section
(b) Magnified view of coating cross section.

Figure 2.—Scanning electron microscope photomicrograph of cross section of metalized graphite, after firing in dry hydrogen at 1600 °C, shows good coverage and bonding.

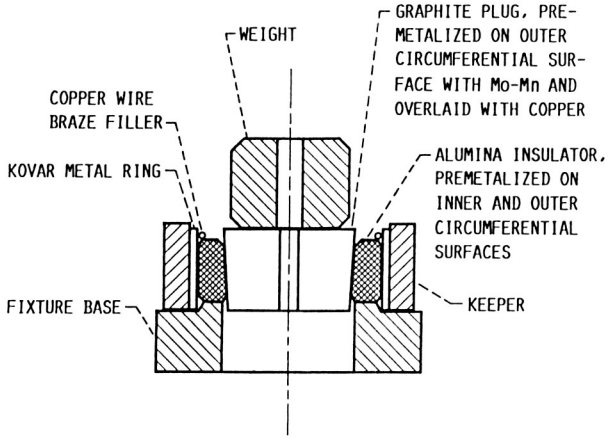

Figure 3.—Typical collector electrode module with fixturing prior to dry hydrogen brazing with copper braze filler metal.

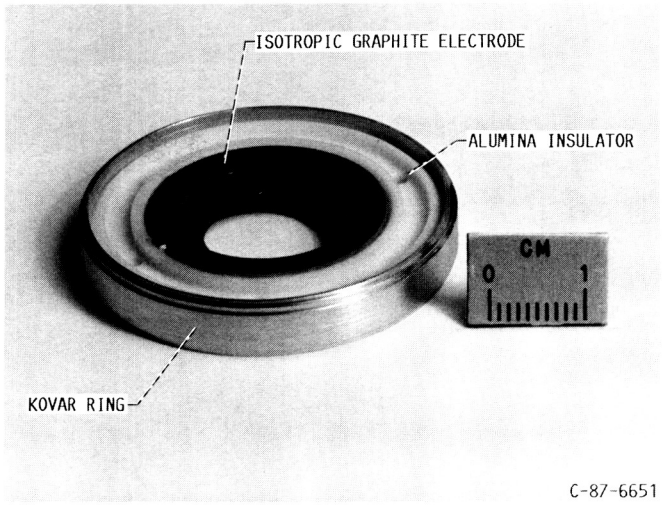

Figure 4.—Typical all-brazed electrode module showing isotropic graphite electrode, alumina insulator, and Kovar-metal outer ring.

made up the entire MDC assembly, except for internal wiring and ion pump, are shown in figure 5. The modules, together with the HV feedthrough assembly and TWT output flange, were stacked to create the multiple-tiered arrangement shown in figure 6 and were joined by electron beam welds to make the final vacuum-tight enclosure. The finished MDC assembly, joined to the TWT body by welds and mounted onto the baseplate, is shown in figure 7.

Performance Optimization and Evaluation

A performance optimization system was used to optimize the TWT overall and MDC efficiencies for broadband operation at saturation. This system provides a real-time readout of the recovered power P_{rec} on a digital voltmeter (DVM), as any of the system variables are changed while the TWT-MDC is operating. This optimization system was first used in the final focusing of the PPM stack of the TWT. Parameters P_{rec}, total body current I_G, and P_{RF} were monitored during this operation. It had been previously observed that (even at constant P_{RF}) the addition of shunts which lowered I_G did not necessarily increase P_{rec}; however, locations for shunts could be found where both I_G and P_{rec} improved. In the present case the final focusing was used to boost the RF output power by 1 to 2 percent, while slightly increasing P_{rec} and reducing I_G. This resulted in the improvement of the overall efficiency by several percent. After final focusing of the tube, TWT-MDC performance optimization was limited to optimization of the MDC operating voltages for broadband operation at saturation. Optimization of the refocusing system by trimming the strength of the two permanent magnets was not attempted, since very good results were obtained at the nominal values.

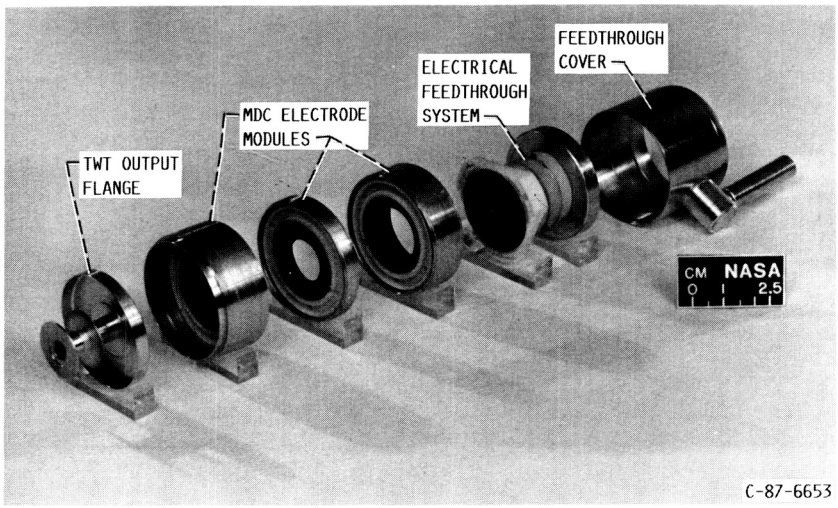

Figure 5.—Exploded view of four-stage, isotropic graphite electrode depressed collector ready for final assembly by welding.

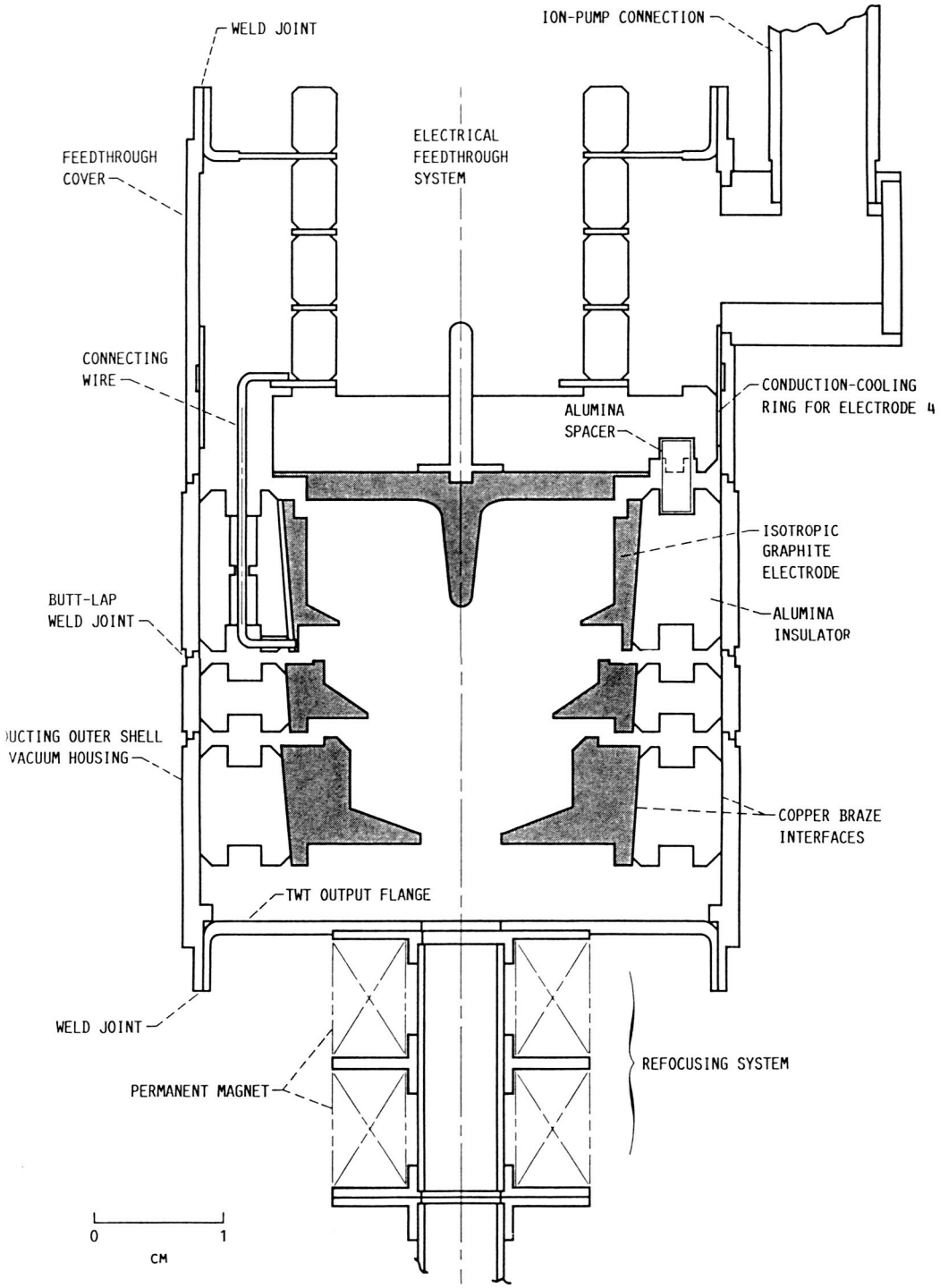

Figure 6.—Cross section of four-stage, brazed, isotropic graphite electrode depressed collector and permanent magnet refocusing sytem.

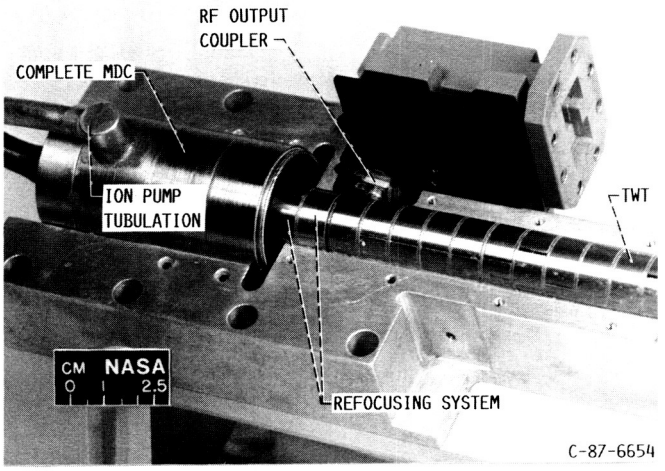

Figure 7.—Fully assembled TWT and collector cradled within a baseplate.

The TWT bodies were added to the MDC's without any previously documented performance (P_{RF} and body power P_b as functions of frequency, and P_b as a function of P_{RF} at a given frequency) with an undepressed collector. Consequently, as discussed in reference 6, the computation of the MDC efficiencies required some assumptions as to the intercepted beam power and circuit losses (the sum of which is P_b) at various operating conditions. In this report it was assumed that the experimental TWT (004) exhibited the same (frequency dependent) beam interception and circuit loss characteristics as model MTZ–7000, serial number 103 (ref. 7), a TWT of virtually identical design. Since the computed collector efficiencies were not based on directly measured values of P_b for the same TWT, they were labeled as "estimated collector efficiencies."

Filtered input drive at the fundamental frequency was used throughout these tests. Saturation was determined by using an uncalibrated power meter which, by means of a low-pass filter, measured RF power only at the fundamental frequency. However, only the total RF power P_{RF} (including any harmonic power) that was dissipated in the water-cooled, matched load was measured, and all TWT overall and electronic efficiencies reported here are based on this P_{RF}.

Results of Bakeout and Processing

The TWT-MDC's were baked out at 500 °C in the production-line facility and processed sequentially. At the outset it was anticipated that the graphite MDC's might require special outgassing treatment. Consequently, the first model (TWT 004) was scheduled for the maximum time allotted (but seldom needed) for production TWT's. The bakeout time for subsequent models was reduced to determine if the extra-long bakeout was really required. The bakeout durations at 500 °C were the following:

(1) TWT 004—72 hr
(2) TWT 005—50 hr
(3) TWT 006—55 hr

All three TWT-MDC's exhibited similar bakeout characteristics. It required 16 to 18 hr to reach 500 °C, and much of the gas evolution took place during this time. By the time 10 hr at 500 °C had passed, the pressure had dropped by about two orders of magnitude from the maximum, and decreased subsequently only very gradually. Overall, in terms of outgassing performance, the TWT-MDC's with graphite MDC's were largely indistinguishable from production model TWT's equipped with copper electrode MDC's.

In subsequent TWT-MDC processing, the 2-liter/s ion pump was used continuously. For the first TWT-MDC (TWT 004), a very conservative pump-current upper limit of 0.1 μA was set to minimize the risk of potentially damaging MDC arcing. This corresponded to a pressure in the upper half of the 10^{-9} torr scale at the pump. For TWT's 005 and 006, when it became apparent that the graphite MDC's were rugged and not easily damaged by arcs (and TWT 004 had already been successfully processed and delivered), the limit was raised to 0.5 μA (3×10^{-8} torr).

TWT 004 was brought up to CW operation after only 40 hr of RF and dc beam processing. Additional aging, CW focusing, and initial TWT-MDC performance evaluation were completed in the subsequent 30 hr at Teledyne MEC. The tube was shipped with a total of 70 hr of pulsed and CW operation. This processing time falls within the acceptable range for the corresponding production model TWT's equipped with copper electrode MDC's.

At NASA Lewis, during the subsequent 30-hr performance optimization and evaluation program, the 2-liter/s pump was used continuously. Typical pump currents were 0.01 to 0.03 μA. At the start of the extended CW test (discussed later in the section Results of Extended CW Test), with the TWT-MDC having accumulated a total of about 100 hr of pulsed and CW operation, the 2-liter/s pump was turned off. The appendage pump was never used, except as a pressure gauge for very short, widely spaced intervals to look for a possible pressure buildup during the extended test. No measurable pump current was ever detected.

TWT's 005 and 006 took 138 and 136 hr, respectively, to come up to CW operation, even with the higher allowed pump current (0.5 μA). Additional time was required for stabilization and evaluation of TWT-MDC performance. Some of the additional processing time required (compared to TWT 004), however, was due to the unattended overnight or weekend operation (when the duty cycle was not increased as the pressure improved). Nevertheless, it appears that the additional day of bakeout time of TWT 004 led to a significant reduction in subsequent processing time. TWT's 005 and 006 have yet to be tested at NASA Lewis.

Comparison of Computed and Measured Results

The MDC design for the TWT's reported here is a refinement of the one produced for TWT MTH-5065, serial number 001 (ref. 8), in an attempt to further reduce the secondary-electron-emission losses in the MDC by better electrostatic suppression of secondaries. The design was revised within the constraints of using the existing passive support structure design of TWT 001 and only machining modified electrode shapes from the same basic modules. (See, e.g., fig. 3.)

The MDC geometry, the applied potentials, and the charge trajectories are shown in figure 1 for the case of experimentally optimized voltages. The computed and measured TWT-MDC performances are compared in detail in table II. Since the tube operating parameters for the analytical case and the experimental TWT (004) differ somewhat, the results are shown as percentages of V_0, I_0, and V_0I_0, where V_0 is the cathode potential with respect to ground and I_0 is the beam current. The experimental circuit and beam interception losses are based on the measured values of body power P_b and intercepted beam current I_B for MTZ-7000, serial number 103 (a TWT of very similar design, whose parameters were

TABLE II.—ANALYTICAL AND EXPERIMENTAL PERFORMANCES OF TWT 004 AND 2.4-cm-DIAMETER, FOUR-STAGE, DEPRESSED COLLECTOR, WITH TWT OPERATING AT SATURATION AT 8.4 GHz IN LOW MODE AND WITH EXPERIMENTALLY OPTIMIZED COLLECTOR VOLTAGES

[Computed trajectories shown in fig. 1. Voltages, currents, and powers given as percentages of V_0, I_0, and V_0I_0, respectively, where V_0 is cathode potential with respect to ground and I_0 is beam current.]

(a) MDC performance

Collecting element	Voltage	Analytical		Experimental	
		Current	Recovered power	Current	Recovered power
TWT body (interception)	0	0	0	3.6	0
TWT body (backstreaming)	0	3.1	0		0
Collector electrode:					
1	54.5	23.8	13.0	35.4	19.3
2	65.6	25.0	16.4	24.7	16.2
3	85.1	46.9	39.9	35.7	30.4
4	100	1.2	1.2	.4	.4
Collector efficiency, η_{col}, percent		83.2		[a]83.8	
Overall efficiency, η_{ov}, percent		45.8		50.4	

(b) Final power distribution

Components of power	Analytical	Experimental
RF output power	13.5	17.0
Total RF power losses (including circuit and sever losses)	1.7	[a]2.8
Beam interception losses	0	1.7
Backstreaming to TWT body	3.1	(b)
MDC dissipation	11.2	(b)
Recovered power	70.5	66.4

[a]Estimated value, based on body power measurements made on a TWT of similar design (model MTZ-7000, serial number 103).
[b]Not measured.

used to model the TWT performance) and an assumed value for the average energy of intercepted current of $eV_0(1-\eta_e)$, where η_e is the electronic efficiency and e is the value of the electronic charge. This yielded a "measured" circuit efficiency η_c of 86 percent, an intercepted beam power of 1.1 percent, and a P_b of 3.8 percent of beam power.

The computed and measured collector efficiencies show very good agreement. The agreement between computed and measured overall efficiencies is not as good because of differences between the computed and measured TWT RF efficiencies. This latter discrepancy is due largely to several design refinements made to the RF structure and to the electron gun design since the basic tube was modeled and analyzed: TWT's 004 to 006 were produced near the end of a lengthy production run. The computed and measured current distributions show reasonably good agreement.

MDC Test Results With TWT 004

TWT-MDC Performance at Saturation

The saturated RF output power and the values of TWT body power P_b, used to compute estimated collector efficiencies, are shown as functions of frequency in figure 8. These estimated values of P_b (based on measured values for a TWT of almost identical design, as discussed in the preceding section) correspond to frequency-dependent beam power interceptions in the range 0.9 to 1.2 percent and TWT circuit efficiencies in the range 80 to 88 percent. The RF and overall efficiencies as functions of frequency are shown in figure 9. The estimated MDC efficiency as a function of frequency is shown in figure 10. The collector efficiency is relatively insensitive to the operating frequency. The results are summarized in table III. The average RF, overall, and collector efficiencies were 14.9, 46.4 and 83.6 percent, respectively.

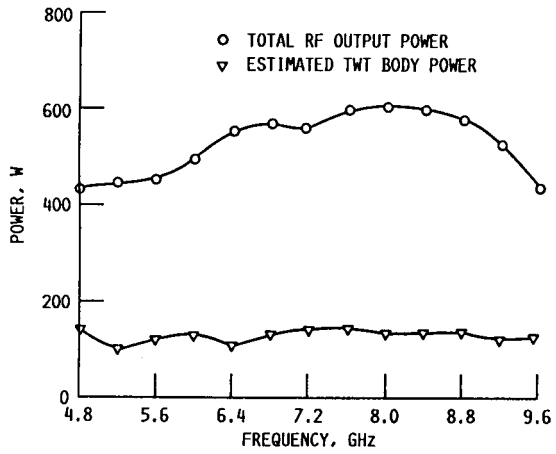

Figure 8.—Total RF output power and estimated body power as functions of frequency at saturation.

The MDC operating voltages, normalized with respect to cathode voltage, are shown in table IV. The TWT-MDC current and dc input power distributions are shown in figures 11 and 12, respectively.

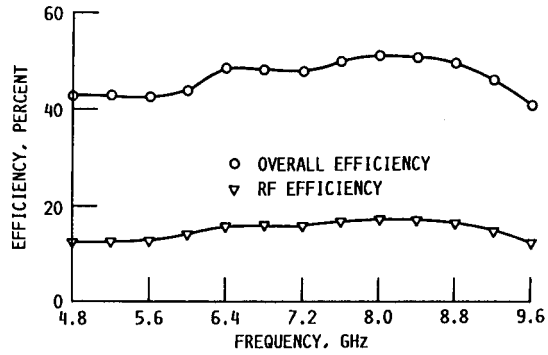

Figure 9.—Overall and RF efficiencies as functions of frequency at saturation.

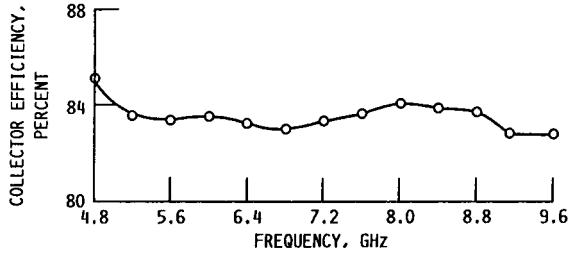

Figure 10.—Estimated collector efficiency as function of frequency at saturation.

TABLE III.—SUMMARY OF TWT AND MDC PERFORMANCE AT SATURATION ACROSS OPERATING BAND OF 4.8 TO 9.6 GHz

Number of MDC stages	4
Average RF efficiency, percent	14.9
Average overall efficiency, percent	46.4
Average estimated collector efficiency, percent	83.6
Maximum dc input power, W	1195

TABLE IV.—MDC OPERATING VOLTAGES NORMALIZED WITH RESPECT TO CATHODE VOLTAGE (OPTIMIZED FOR BROADBAND OPERATION AT SATURATION)

MDC electrode number	Four-stage normalized voltage
1	0.533
2	.667
3	.862
4	1.00

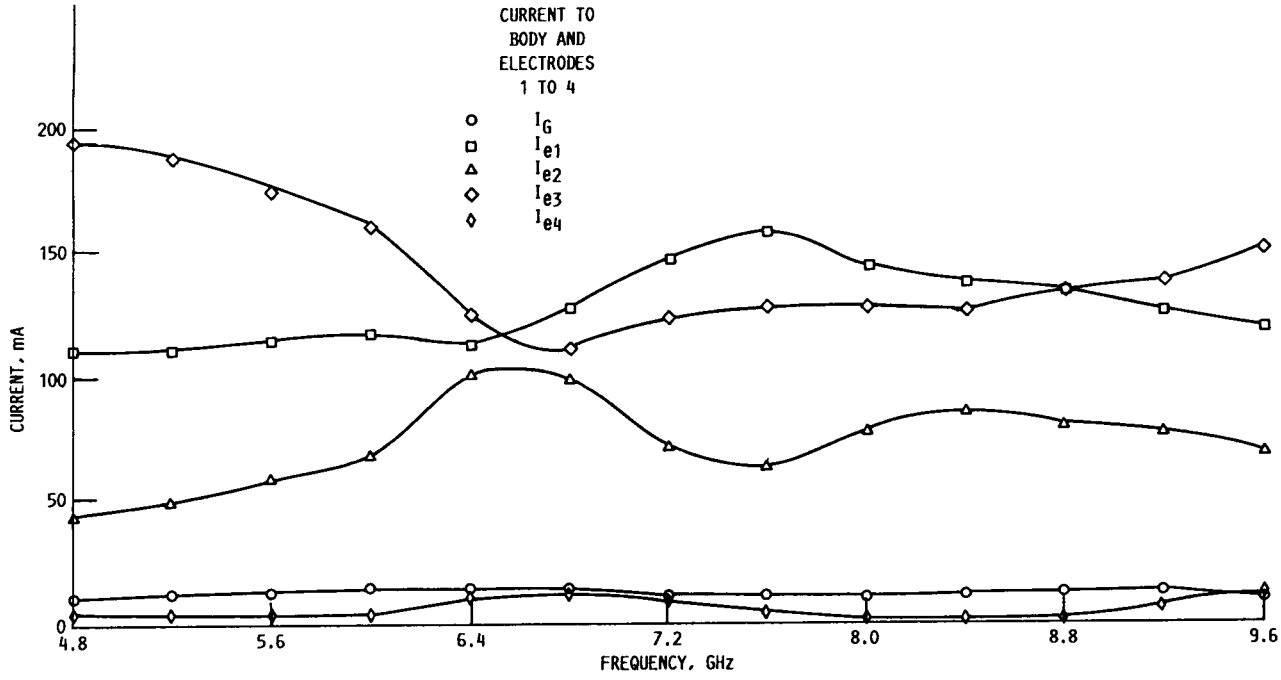

Figure 11.—Four-stage collector electrode current distribution as function of frequency at saturation.

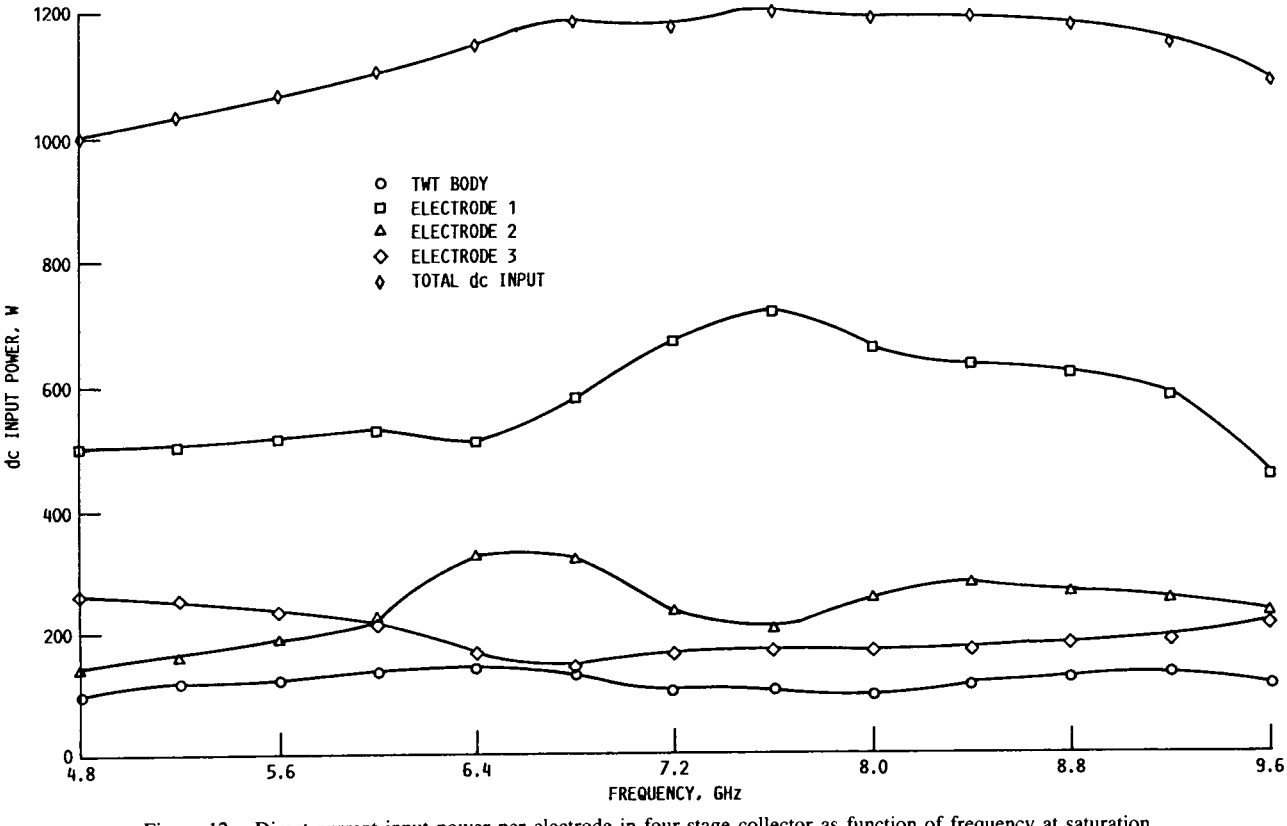

Figure 12.—Direct current input power per electrode in four-stage collector as function of frequency at saturation.

TWT-MDC Performance Over TWT Dynamic Range

The TWT overall efficiency and the collector efficiency as functions of RF output power (at the operating frequency of 8.0 GHz, corresponding to the highest RF efficiency at saturation) are shown in figures 13 and 14, respectively. The MDC operating conditions (voltages) used were identical to those used for saturated operation. The MDC efficiency rose steadily (but very slowly) for TWT operation increasingly below saturation, and a reasonable overall efficiency (>20 percent) could be maintained for TWT operation as much as 6 dB below saturation. The collector efficiency, for operation of the TWT in the low end of the linear range, was severely limited by the potential (0.86 V_0, optimized for saturation) of the second most depressed electrode. No attempt was made to optimize the collector for linear operation of the TWT.

The TWT and MDC current and dc input power distributions as functions of RF output power at 8.0 GHz are shown in figures 15 and 16, respectively. Together with the corresponding distributions at saturation (discussed previously in this section), they define the power conditioning requirements of the TWT-MDC.

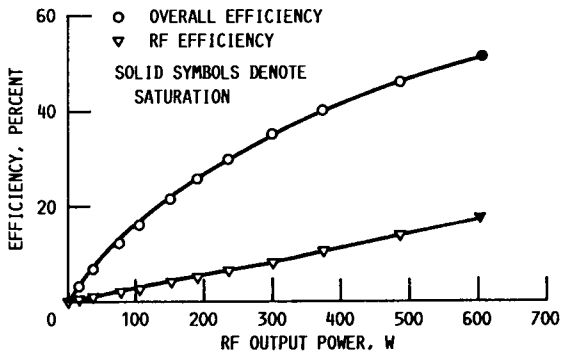

Figure 13.—Overall and RF efficiencies as functions of RF output power at 8.0 GHz.

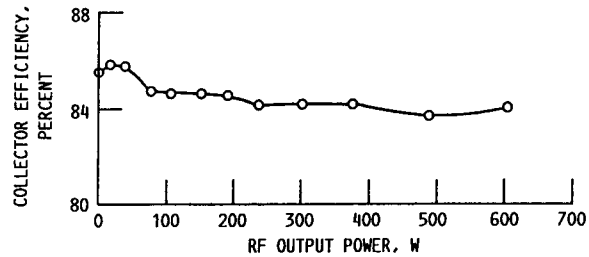

Figure 14.—Estimated collector efficiency as function of RF output power at 8.0 GHz.

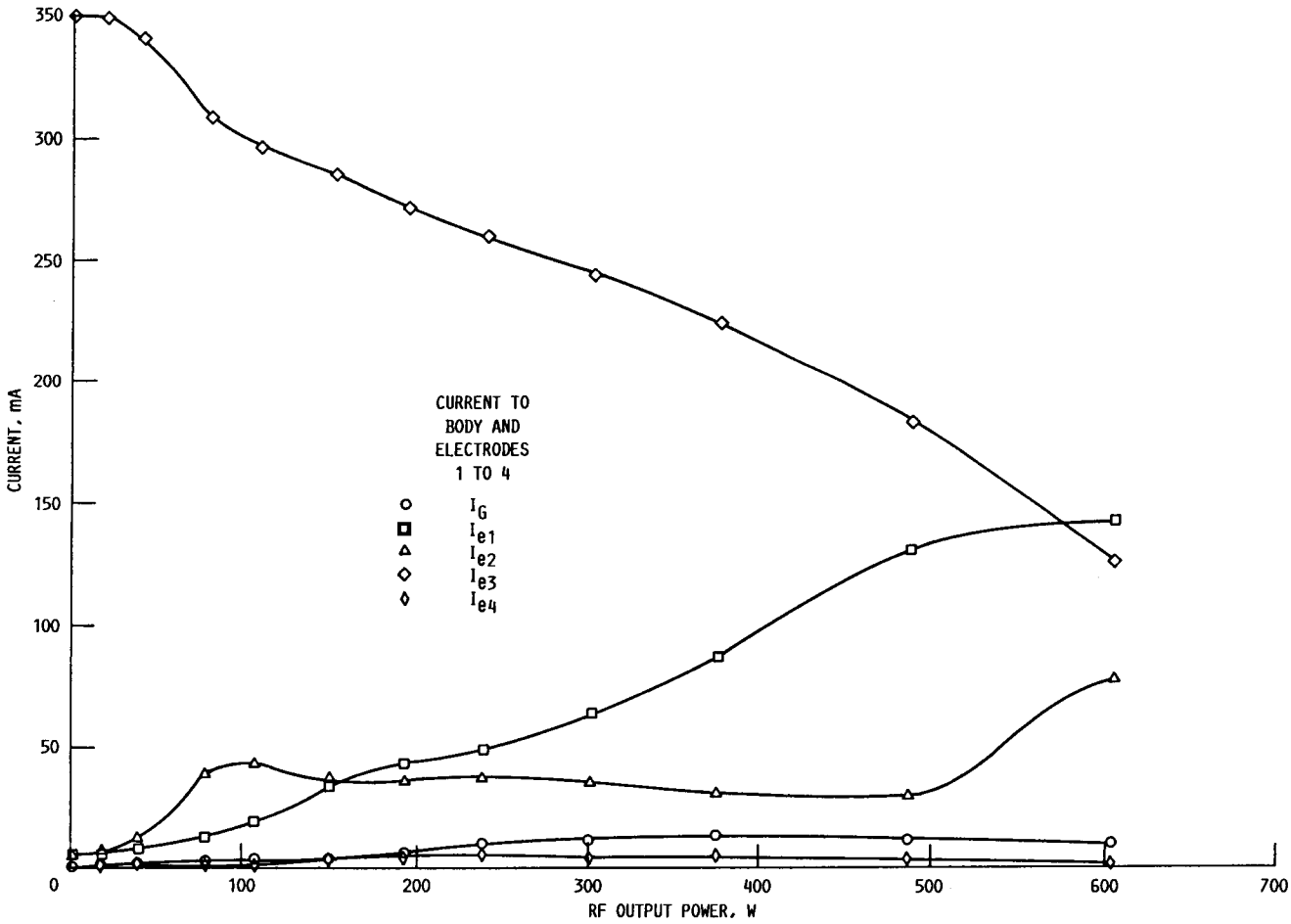

Figure 15.—Four-stage collector current distribution as function of RF output power at 8.0 GHz.

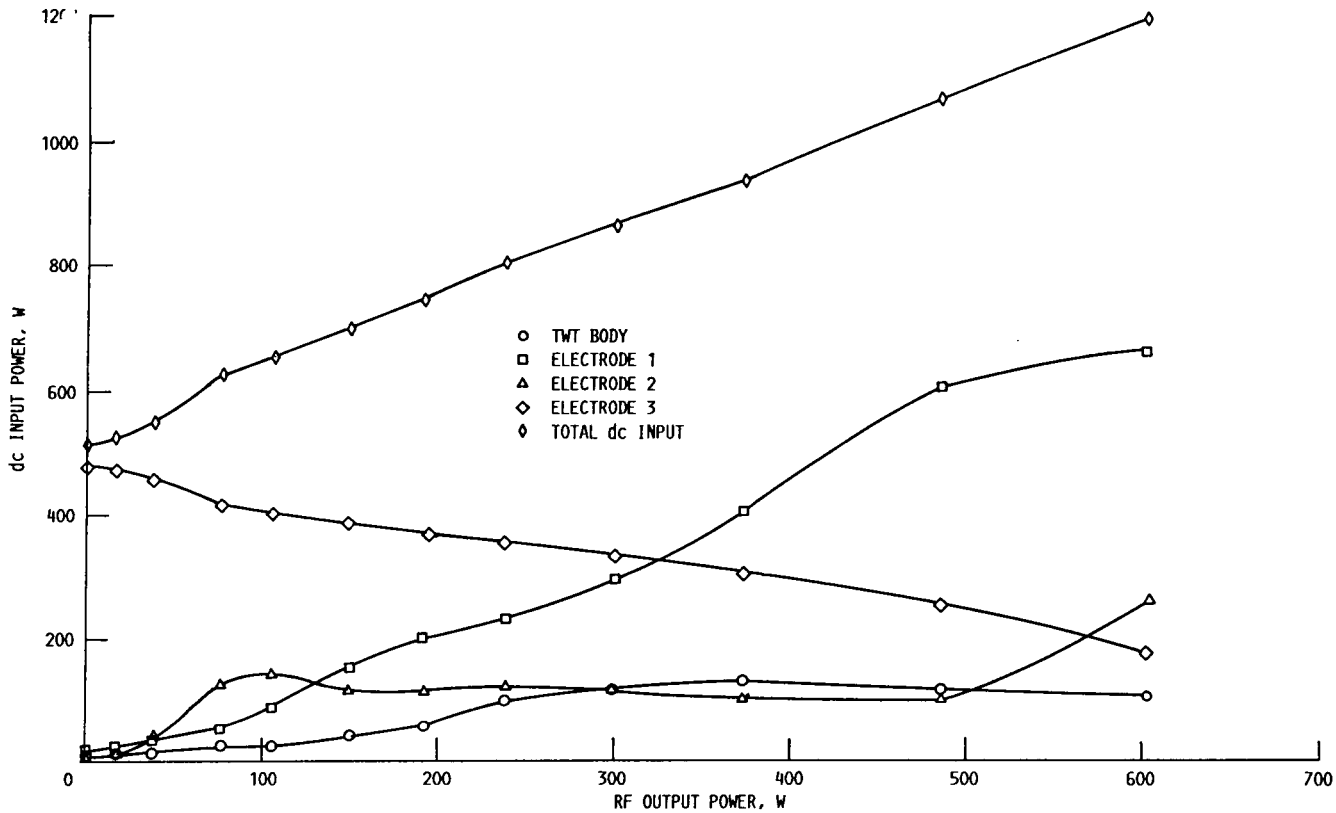

Figure 16.—Direct current input power per electrode in four-stage collector as function of RF output power at 8.0 GHz.

Results of Extended CW Test

The extended test was performed to evaluate the stability of the graphite electrode surfaces under relatively intense long-term electron bombardment. It was conducted largely at the single operating condition shown in table V and was of 1500-hr duration. Operation below saturation (which places less stress on the TWT itself) was selected to minimize the risk of TWT performance changes. The TWT-MDC performance was monitored on a daily basis. In addition, at the beginning of the test and at 500-hr intervals thereafter, carefully calibrated TWT-MDC performance was obtained at a number of selected RF output power levels at 8.0 GHz. These were saturated output, 575, 550, 500, and 0 W (dc beam). During the test the TWT-MDC was subjected to more than 50 on/off cycles of the electron beam.

Table VI presents a detailed comparison of the TWT-MDC performance at the beginning and the end of the test, for three of the five monitored operating conditions. Considerable care had to be taken to reproduce the RF output power levels very precisely, since the MDC current distribution was highly sensitive to P_{RF}. In general, the TWT-MDC performance was very stable over the 1500-hr interval. The very slight improvement in the TWT and MDC performance (increased P_{rec}) was due largely to a decrease in the total body current I_G. The observed small (but consistent) increase in the net current collected by electrode 4 suggests that the lower body current at the end of the test may be due to slightly lower levels

TABLE V.—TYPICAL TWT-MDC OPERATING CONDITIONS DURING EXTENDED CW TEST OF TWT 004

[Cathode potential, V_0, 9.75 kV; beam current, I_0, 0.36 A; frequency, 8.0 GHz.]

Total RF output power, P_{RF}, W	550
Total body current, I_G, mA	8
Current to electrodes 1 to 4, mA	
I_{e1}	146
I_{e2}	48
I_{e3}	154
I_{e4}	4
Estimated total MDC dissipation, W	500
MDC voltages (See table IV.)	Nominal

TABLE VI.—TWT-MDC PERFORMANCE EARLY IN CW TEST AND AT END OF EXTENDED CW RF TEST OF TWT 004

[Cathode potential, V_0, 9.75 kV; beam current, I_0, 0.36 A; $t = 0$ corresponds to time of delivery of TWT to NASA Lewis.]

(a) 8.0 GHz, saturation

TWT parameter	At $t \approx 30$ hr	At $t \approx 1540$ hr
Total RF output power, P_{RF}, W	597	597
Total body current, I_G, mA	8.6	7.7
Current to electrodes 1 to 4, mA		
I_{e1}	142.9	141.7
I_{e2}	78.7	81.0
I_{e3}	127.9	127.4
I_{e4}	1.9	2.3
Recovered power, P_{rec}, W	2319	2328
Total dc input power, W	1191	1184
Overall efficiency, η_{ov}, percent	50.1	50.4

(b) 8.0 GHz, $P_{RF} = 550$ W

TWT parameter	At $t \approx 30$ hr	At $t \approx 1540$ hr
Total RF output power, P_{RF}, W	550	550
Total body current, I_G, mA	7.8	6.9
Current to electrodes 1 to 4, mA		
I_{e1}	145.9	145.5
I_{e2}	48.2	49.6
I_{e3}	154.2	153.8
I_{e4}	3.8	4.2
Recovered power, P_{rec}, W	2375	2383
Total dc input power, W	1135	1127
Overall efficiency, η_{ov}, percent	48.5	48.8

(c) Direct current beam

TWT parameter	At $t \approx 30$ hr	At $t \approx 1540$ hr
Total RF output power, P_{RF}, W	0	0
Total body current, I_G, mA	1.0	0.3
Current to electrodes 1 to 4, mA		
I_{e1}	4.2	4.2
I_{e2}	3.8	4.6
I_{e3}	351.0	351.1
I_{e4}	0	0
Recovered power, P_{rec}, W	2995	3000
Total dc input power, W	515	513

of backstreaming secondary-electron current from the collector. The results at RF power levels of 575 and 500 W were very similar, with slightly lower I_G's and slightly higher values for P_{rec}.

As discussed in the section Results of Bakeout and Processing, except for very short duration, widely spaced, operation of the appendage pump to look for possible pressure buildups, neither ion pump was used during the test. No measurable pump current was ever detected during the pressure monitoring operation.

Concluding Remarks

The bakeout and processing (outgassing) performances of small-sized isotropic graphite MDC's were evaluated in conjunction with 500-W, CW, octave bandwidth TWT's and compared to production TWT's equipped with copper electrode MDC's. The results suggest that an extended bakeout of the graphite MDC's can lead to significantly reduced subsequent processing times, comparable to those required with copper electrode MDC's. It was demonstrated that TWT's equipped with isotropic graphite MDC's need not require even small appendage ion pumps. The use of BeO in place of the alumina MDC insulators for this and higher power TWT applications would result in significantly reduced graphite operating temperatures and possibly in reduced outgassing requirements and processing times.

The improved single-step brazing technique (which is compatible with commonly available hydrogen brazing furnaces) can significantly simplify graphite electrode MDC fabrication, especially on a production-line basis. The copper-braze MDC assembly is readily compatible with a higher (e.g., 550 °C) bakeout, which could further reduce the TWT-MDC processing time. Further investigations, however, are needed to optimize the brazing techniques.

The computer-aided design technique was used to fine-tune an already highly efficient MDC design. The TWT-MDC performed well. The average overall and MDC efficiencies for saturated operation across the octave bandwidth were 46.4 and 83.6 percent, respectively. The extended CW test showed excellent stability of the isotropic graphite electrode surfaces, and outgassing levels sufficiently low that not even an appendage ion pump was required.

The results are encouraging. The isotropic graphite shows considerable promise as an MDC electrode material because of its high purity, low-cost potential for very compact overall MDC size, and relatively low secondary-electron-emission yield characteristics. Nevertheless, considerably more test experience is required before definitive conclusions on its suitability for high-risk space TWT applications can be made. The isotropic graphite MDC technology, however, seems to be sufficiently advanced to proceed with certain airborne applications.

Lewis Research Center
National Aeronautics and Space Administration
Cleveland, Ohio, December 15, 1988

References

1. Ramins, P., et al.: Verification of an Improved Computational Design Procedure for TWT-Dynamic Refocuser MDC Systems with Secondary Electron Emission Losses. IEEE Trans. Electron Devices, vol. 33, no. 1, Jan. 1986, pp. 85-90.
2. Curren, A.N.: Carbon and Carbon-Coated Electrodes of Multistage Depressed Collectors for Electron-Beam Devices—A Technology Review. IEEE Trans Electron Devices, vol. 33, no. 11, Nov. 1986, pp. 1902-1914.
3. Ebihara, B.T.; and Ramins, P.: Design, Fabrication and Performance of Small, Graphite Electrode, Multistage Depressed Collectors With 200-W CW, 8- to 18-GHz Traveling-Wave Tubes. NASA TP-2693, 1987.
4. Ramins P.; and Ebihara B.T.: Improvements in MDC and TWT Overall Efficiency Through the Application of Carbon Electrode Surfaces. IEEE Trans. Electron Devices, vol. 33, no. 11, Nov. 1986, pp. 1915-1924.
5. Ramins, P., et al.: Performance of a Small, Graphite Electrode, Multistage Depressed Collector With a 500-W, Continuous Wave, 4.8- to 9.6-GHz Traveling Wave Tube. NASA TP-2788, 1988.
6. Kosmahl, H.G.: Comments on Measuring the Overall and the Depressed Collector Efficiency in TWT's and Klystron Amplifiers. IEEE Trans. Electron Devices, vol. 26. no. 2, Feb. 1979, p. 156.
7. Ramins, P.; and Fox, T.A.: Multistage Depressed Collector with Efficiency of 90 to 94 Percent for Operation of a Dual-Mode Traveling Wave Tube in the Linear Region. NASA TP-1670, 1980.
8. Ramins, P.; Force, D.A.; and Kosmahl, H.G.: Analytical and Experimental Performance of a Dual-Mode Traveling-Wave Tube and Multistage Depressed Collector. NASA TP-2752, 1987.

NASA
National Aeronautics and Space Administration

Report Documentation Page

1. Report No.	2. Government Accession No.	3. Recipient's Catalog No.
NASA TP-2904		

4. Title and Subtitle

Design, Fabrication, and Performance of Brazed, Graphite Electrode, Multistage Depressed Collectors With 500-W, Continuous Wave, 4.8- to 9.6-GHz Traveling-Wave Tubes

5. Report Date

March 1989

6. Performing Organization Code

7. Author(s)

Peter Ramins and Ben Ebihara

8. Performing Organization Report No.

E-4361

10. Work Unit No.

506-44-21

9. Performing Organization Name and Address

National Aeronautics and Space Administration
Lewis Research Center
Cleveland, Ohio 44135-3191

11. Contract or Grant No.

13. Type of Report and Period Covered

Technical Paper

12. Sponsoring Agency Name and Address

National Aeronautics and Space Administration
Washington, D.C. 20546-0001

14. Sponsoring Agency Code

15. Supplementary Notes

16. Abstract

A small, isotropic graphite electrode, multistage depressed collector (MDC) was designed, fabricated, and evaluated in conjunction with a 500-W, continuous wave (CW), 4.8- to 9.6-GHz traveling-wave tube (TWT). The carbon electrode surfaces were used to improve the TWT overall efficiency by minimizing the secondary-electron-emission losses in the MDC. The design and fabrication of the brazed graphite MDC assembly are described. The brazing technique, which used copper braze filler metal, is compatible with both vacuum and the more commonly available hydrogen atmosphere brazing furnaces. The TWT and graphite electrode MDC bakeout, processing, and outgassing characteristics were evaluated and found to be comparable to TWT's equipped with copper electrode MDC's. The TWT and MDC performance was optimized for broadband CW operation at saturation. The average radiofrequency (RF), overall, and MDC efficiencies were 14.9, 46.4, and 83.6 percent, respectively, across the octave operating band. A 1500-hr CW test, conducted without the use of an appendage ion pump, showed no gas buildup and excellent stability of the electrode surfaces.

17. Key Words (Suggested by Author(s))	18. Distribution Statement
Traveling-wave tube Multistage depressed collector Graphite electrodes Brazed graphite assembly	Unclassified – Unlimited Subject Category 33

19. Security Classif. (of this report)	20. Security Classif. (of this page)	21. No of pages	22. Price*
Unclassified	Unclassified	18	A03

NASA FORM 1626 OCT 86

*For sale by the National Technical Information Service, Springfield, Virginia 22161

NASA-Langley, 1989